

# Quark running mass and vacuum energy density in truncated Coulomb gauge QCD for five orders of magnitude of current masses

P. Bicudo

*CFTP, Departamento de Física, Instituto Superior Técnico,  
Avenida Rovisco Pais, 1049-001 Lisboa, Portugal*

---

## Abstract

We study in detail the effect of the finite current quark mass on chiral symmetry breaking, in the framework of truncated Coulomb gauge QCD with a linear confining quark-antiquark potential. In the chiral limit of massless current quarks, the breaking of chiral symmetry is spontaneous. But for a finite current quark mass, some dynamical symmetry breaking continues to add to the explicit breaking caused by the quark mass. Moreover, using as order parameter the mass gap, i. e. the quark mass at vanishing moment or the quark condensate, a finite quark mass transforms the chiral symmetry breaking from a phase transition into a crossover. For the study of the QCD phase diagram it thus is relevant to determine how the current quark mass affects chiral symmetry breaking. Since the current quark masses of the six standard flavours  $u, d, s, c, b, t$  span over five orders of magnitude from 1.5 MeV to 171 GeV, we develop an accurate numerical method to study the running quark mass gap and the quark vacuum energy density from very small to very large current quark masses.

*Key words:* `elsart`, quark mass, chiral symmetry breaking, vacuum energy density

*PACS:* 11.30.Rd, 12.39.-x, 12.38.Aw, 12.15.Ff

---

## 1 Introduction

Chiral symmetry breaking has been studied in detail with chiral invariant *and confining* quark models in the chiral limit of a vanishing current quark mass  $m_0$ . For a finite current quark mass  $m_0 \neq 0$ , studies exist with an approximate

---

*Email address:* `bicudo@ist.utl.pt` (P. Bicudo).

confinement [1,2,3,4] or with a quadratic confining potential [7,6,5], but very few studies have been performed [8,9] with an exactly linear confining potential. Since the current quark masses of the six standard flavours  $u, d, s, c, b, t$  span over five orders of magnitude from 1.5 MeV to 171 GeV, here we develop a new numerical method to study the quark mass gap and the quark vacuum energy density, with a linear exactly confining potential, from very small to very large quark masses.

Notice that even in the chiral limit of  $m_0 = 0$ , the quark has a constituent running mass  $m(p)$  function of the momentum  $p$ , solution of the mass gap equation (equivalent to the Schwinger-Dyson equation) for the quark. Recently we have shown how to measure in the excited hadron spectra the running mass  $m(p)$  [10]. The chiral invariant and confining quark models have also been applied to phase studies at finite temperature  $T$  and chemical potential  $\mu$  [11,12,13,14,15,16,17,18]. A finite quark mass is relevant both for the study of hadrons which have been investigated for decades, and for the study the QCD phase diagram which will be explored in the future at RHIC, LHC and FAIR. In the phase diagram, a finite current quark mass  $m_0$  affects the position of the critical point between the crossover at low chemical potential  $\mu$  and the phase transition at higher  $\mu$ . Moreover the current quark mass affects the QCD vacuum energy density  $\mathcal{E}$ , relevant for the dark energy of cosmology. This all occurs in the dynamical generation of the quark mass  $m(p)$ . While the quark condensate  $\langle\bar{\psi}\psi\rangle$  is a frequently used order parameter for chiral symmetry breaking, the mass gap, *i. e.* the quark mass at vanishing momentum  $m(0)$  is another possible order parameter for chiral symmetry breaking. However, due to technical difficulties,  $m(0)$  has not been computed in detail previously in confining and chiral invariant quark models.

Here we study in detail how a finite current quark mass  $m_0 \neq 0$  affects the dynamically generated quark mass  $m(p)$ . We utilize the linear confining potential for the quark-antiquark interaction, in the chiral quark model or Coulomb Gauge quark model, including both confinement and chiral symmetry. While this model, in the framework Coulomb gauge Hamiltonian formalism is not yet full QCD, it is presently the only model able to include both the quark-antiquark confining potential and quark-antiquark vacuum condensation. Importantly, since our model is well defined and solvable, it can be used as a simpler model than QCD, and yet qualitatively correct, to address different aspects of hadronic physics. It is adequate to study the QCD phase diagram microscopically [11,12,13,14,15,16,17,18]. We scan the current quark masses, from the light quarks to the heavy quarks, computing the running quark mass  $m(p)$  with detail, including the infrared limit of  $m(0)$ , *i. e.* the mass gap.

In Section II we derive in detail the mass gap equation. In Section III we review the numerical difficulties of this non-linear integral equation, with cancelling infrared divergences. We solve the mass gap equation with a new numerical

method, dedicated to determine in detail the difficult infrared region of small momentum  $p \simeq 0$ . In Section IV we discuss our results and conclude.

## 2 Our framework

### 2.1 Possible link to QCD.

Our framework can be approximately derived from QCD, in two different gauges. In Coulomb gauge  $\nabla \cdot \mathbf{A}(\mathbf{x}, t) = 0$  the interaction potential, has been derived by Lee, [19], and by Szczepaniak and Swanson [20,21]. In the present study we address the quark fields only and thus  $V_I$  reduces to the quark part of the density-density term,

$$V_I = + \frac{1}{2} g^2 \int d\mathbf{x} d\mathbf{y} \mathcal{J}^{-1} \psi^\dagger(\mathbf{x}) T^a \psi(\mathbf{x}) \langle \mathbf{x}, a | \times (\nabla \cdot \mathbf{D})^{-1} (-\nabla^2) (\nabla \cdot \mathbf{D})^{-1} | \mathbf{y}, b \rangle \mathcal{J} \psi^\dagger(\mathbf{y}) T^b \psi(\mathbf{y}) \quad (1)$$

The covariant derivative in the adjoint representation  $\mathbf{D} = \nabla - g\mathbf{A}$ , and  $\mathcal{J} = \text{Det}[\nabla \cdot \mathbf{D}]$  contribute to the density-density interaction, which is expected to be confining in QCD.

Another approximate path from QCD to our model considers the modified coordinate gauge of Balitsky [22],  $\mathbf{A}(\mathbf{0}, t) = 0$ ,  $\mathbf{x} \cdot \mathbf{A}(\mathbf{x}, t) = 0$  and in the interaction potential for the quark sector,

$$V_I = \int d^3x \left[ \psi^\dagger(x) (m_0\beta - i\vec{\alpha} \cdot \vec{\nabla}) \psi(x) + \frac{1}{2} g^2 \int d^4y \bar{\psi}(x) \gamma^\mu \frac{\lambda^a}{2} \psi(x) \langle A_\mu^a(x) A_\nu^b(y) \rangle \bar{\psi}(y) \gamma^\nu \frac{\lambda^b}{2} \psi(y) + \dots \right] \quad (2)$$

retains the first cumulant order, of two gluons [23,24,25]  $g^2 \langle A_\mu^a(x) A_\nu^b(y) \rangle$  and this also results in a simple density-density harmonic effective confining interaction. As in QCD, this only has one scale.

Thus our framework is similar to an expansion of the QCD interaction, truncated to the leading density-density term. Moreover, to address phenomenology where the meson spectrum fits in linear Regge trajectories, one also needs to assume that the confining quark-antiquark potential is a linear potential. Notice that the short range Coulomb potential could also be included in the interaction, but here we ignore it since it only affects the quark mass through

ultraviolet renormalization [26], which is assumed to be already included in the current quark mass. While this is not exactly equivalent to QCD, our framework maintains three interesting aspects of non-perturbative QCD, a chiral invariant quark-antiquark interaction, [27,28,29,30,31,32] the cancellation of infrared divergences [7,6,5] and a quark-antiquark linear potential [8,9,20,33,34,35,36].

## 2.2 Deriving the mass gap equation

We derive the mass gap equation, where constituent quarks acquire the constituent mass  $m(k)$  [37] in the true and stable vacuum, solving the Schwinger-Dyson equation for the quark propagator,

$$\mathcal{S}^{-1}(p) = \mathcal{S}_0^{-1}(p) - \text{diagram} \quad (3)$$

The diagram is a loop with a solid line on the bottom and a dotted line on the top, with momentum  $k$  on the solid line and  $p-k$  on the dotted line.

We utilize the truncated Schwinger-Dyson equation at the Rainbow level, where the dotted line represents the same density-density interaction  $V_I$  resulting identically from the truncation of Coulomb gauge QCD or of Balitsky gauge QCD. This leads to the same mass gap equation and quark dispersion relation obtained assuming a quark-antiquark  $^3P_0$  condensed vacuum, computing the vacuum energy density with the Hamiltonian, and minimizing the energy density. The relativistic invariant Dirac-Feynman [31] propagators  $\mathcal{S}$ , can be decomposed in the quark and antiquark Bethe-Goldstone propagators [37],

$$\begin{aligned} \mathcal{S}(k_0, \vec{k}) &= \frac{i}{\not{k} - m + i\epsilon} \\ &= \frac{i}{k_0 - \sqrt{k^2 + m^2} + i\epsilon} \sum_s u_s u_s^\dagger \beta - \frac{i}{-k_0 - \sqrt{k^2 + m^2} + i\epsilon} \sum_s v_s v_s^\dagger \beta, \end{aligned} \quad (4)$$

where  $m$  is the quark mass and where the quark spinor  $u_s$  and antiquark spinor  $v_s$  are,

$$\begin{aligned} u_s(\mathbf{k}) &= \left[ \sqrt{\frac{1+S}{2}} + \sqrt{\frac{1-S}{2}} \hat{k} \cdot \vec{\sigma} \gamma_5 \right] u_s(0) \\ v_s(\mathbf{k}) &= \left[ \sqrt{\frac{1+S}{2}} - \sqrt{\frac{1-S}{2}} \hat{k} \cdot \vec{\sigma} \gamma_5 \right] v_s(0), \end{aligned} \quad (5)$$

where  $S = m/\sqrt{k^2 + m^2}$  is a function of the quark mass.

Importantly, in the free propagator, the correct quark propagator in the non condensed vacuum, the quark mass  $m$  is equal to the *current quark mass*  $m_0$ . And it is this current quark mass  $m_0$  which effects in the current quark mass we study in great detail. However when chiral symmetry breaking occurs,  $m$  is not determined from the onset. In the physical vacuum, the *constituent quark mass*  $m(k)$ , is a function of the momentum, a dynamical solution of the mass gap equation.

Replacing the propagator of eq. (5) in the Schwinger-Dyson equation and projecting it with the spinors, we get the mass gap equation and the quark dispersion relation,

$$0 = u_s^\dagger(k) \left\{ k\hat{k} \cdot \boldsymbol{\alpha} + m_0\beta - \int \frac{dk_0'}{2\pi} \frac{d^3\mathbf{k}'}{(2\pi)^3} i\tilde{V}(k-k')\mathcal{S}(k_0', \vec{k}') \right\} v_{s''}(k) \quad (6)$$

$$E(k) = u_s^\dagger(k) \left\{ k\hat{k} \cdot \boldsymbol{\alpha} + m_0\beta - \int \frac{dk_0'}{2\pi} \frac{d^3\mathbf{k}'}{(2\pi)^3} i\tilde{V}(k-k')\mathcal{S}(k_0', \vec{k}') \right\} u_s(k),$$

where the usual notation for Dirac matrices is assumed. Writing the running mass in terms of a sine and a cosine of  $\varphi(k) = \arctan \frac{k}{m(k)}$ , the *chiral angle*,

$$S(k) = \sin \varphi(k) = \frac{m(k)}{\sqrt{k^2 + m(k)^2}},$$

$$C(k) = \cos \varphi(k) = \frac{k}{\sqrt{k^2 + m(k)^2}}, \quad (7)$$

the mass gap equation and the quark energy are,

$$0 = +S(p) B(p) - C(p) A(p) \quad (8)$$

$$E(p) = +S(p) A(p) + C(p) B(p) \quad (9)$$

where the propagator functions  $A$  and  $B$ , respectively replacing the quark mass  $m$  and quark momentum  $|\mathbf{p}|$  in the one-loop dressed quark propagator of eq. (4) are,

$$A(p) = m_0 + \frac{1}{2} \int \frac{d^3\mathbf{k}}{(2\pi)^3} \tilde{V}(\mathbf{p} - \mathbf{k}) S(k),$$

$$B(p) = p + \frac{1}{2} \int \frac{d^3\mathbf{k}}{(2\pi)^3} \tilde{V}(\mathbf{p} - \mathbf{k}) (\hat{p} \cdot \hat{k}) C(k). \quad (10)$$

Equivalently to solve the non-linear integral mass gap equation (8), we can alternatively minimize the vacuum energy density per unit volume,

$$\mathcal{E} = -\frac{g}{2} \int \frac{d^3 \mathbf{p}}{(2\pi)^3} S(p) [A(p) + m_0] + C(p) [B(p) + p] \quad (11)$$

where  $g = N_f N_s N_c$  is the degeneracy factor counting the number of different but degenerate quarks.  $N_s = 2$  is the number of spins and  $N_c = 3$  is the number of colours.  $N_f$  is the number of degenerate flavours, but since each quark has a different current quark mass  $m_0$  one should compute separately the vacuum energy difference for each quark flavour.

### 2.3 The mass gap equation for a linear confining potential

Notice that in the case of a linear potential, divergent in the infrared limit of large  $r$ , the Fourier transform needs an infrared regulator  $\mu$ . A possible form of the linear potential,

$$V(r) = -\sigma \frac{e^{-\mu r}}{\mu} \simeq -\frac{\sigma}{\mu} + \sigma r - \frac{\sigma \mu}{2} r^2 + \dots \quad (12)$$

corresponds, in the limit of small infrared regulator  $\mu$ , to a model of linear confinement where the quark also has an infinite binding energy  $-\frac{\sigma}{\mu}$ . While other infrared regulations can be used for the linear potential, say  $V(r) = \sigma r e^{-\mu r}$  which has no infrared divergent binding energy, the infrared divergent constant of Eq. (12) is exactly cancelled in the mass gap equation by the factor in the integrand  $[S(k)C(p) - S(p)C(k)\hat{k} \cdot \hat{p}]$ . The potential in Eq. (12) has a simple three-dimensional Fourier transform,

$$V(k) = \sigma \frac{-8\pi}{(k^2 + \mu^2)^2}, \quad (13)$$

and this is the momentum space potential frequently utilized to account for linear confinement.

The integrals in the angular variable  $\omega$  of Eq. (10) are,

$$\begin{aligned} \int_{-1}^1 d\omega \frac{-8\pi}{(k^2 + p^2 + 2kp\omega + \mu^2)^2} &= \frac{-16\pi}{[(k-p)^2 + \mu^2][(k+p)^2 + \mu^2]}, \\ \int_{-1}^1 d\omega \frac{-8\pi \omega}{(k^2 + p^2 + 2kp\omega + \mu^2)^2} & \end{aligned} \quad (14)$$

$$= \frac{-16\pi}{(2kp)^2} \left\{ -\frac{2kp(k^2 + p^2 + \mu^2)}{[(k-p)^2 + \mu^2][(k+p)^2 + \mu^2]} + \frac{1}{2} \log \left[ \frac{(k+p)^2 + \mu^2}{(k-p)^2 + \mu^2} \right] \right\} .$$

We find for the propagator functions  $A$  and  $B$ ,

$$\begin{aligned} A(p) &= m_0 - \frac{\sigma}{p^2} \int_0^\infty \frac{dk}{2\pi} I_A(k, p, \mu) S(k) , \\ I_A(k, p, \mu) &= \frac{pk}{(p-k)^2 + \mu^2} - \frac{pk}{(p+k)^2 + \mu^2} , \\ B(p) &= p - \frac{\sigma}{p^2} \int_0^\infty \frac{dk}{2\pi} I_B(k, p, \mu) C(k) , \\ I_B(k, p, \mu) &= \frac{pk}{(p-k)^2 + \mu^2} + \frac{pk}{(p+k)^2 + \mu^2} + \frac{1}{2} \log \frac{(p-k)^2 + \mu^2}{(p+k)^2 + \mu^2} , \end{aligned} \quad (15)$$

leading to the mass gap equation in the two equivalent forms of a non-linear integral functional equation,

$$\begin{aligned} 0 &= pS(p) - m_0C(p) - \frac{\sigma}{p^2} \int_0^\infty \frac{dk}{2\pi} [ \\ &\quad I_A(k, p, \mu) S(k)C(p) - I_B(k, p, \mu) S(p)C(k) ] , \end{aligned} \quad (16)$$

and of a minimum equation of the energy density,

$$\begin{aligned} \mathcal{E} &= \frac{-g}{2\pi} \int_0^\infty \frac{dp}{2\pi} \left[ 2p^3 C(p) + 2p^2 m_0 S(p) + \sigma \times \right. \\ &\quad \left. \int_0^\infty \frac{dk}{2\pi} I_A(k, p, \mu) S(k)S(p) + I_B(k, p, \mu) C(p)C(k) \right] . \end{aligned} \quad (17)$$

Eq. (16) can be rewritten as a fixed point equation for the quark mass function  $m(k)$ ,

$$m(p) = m_0 + \frac{\sigma}{p^3} \int_0^\infty \frac{dk}{2\pi} \frac{I_A(k, p, \mu) m(k)p - I_B(k, p, \mu) m(p)k}{\sqrt{k^2 + m(k)^2}} . \quad (18)$$

Since the potential has an infinite constant independent of the mass, in the variational equation we search for the extremum of the energy difference

$$\begin{aligned}
\mathcal{E} - \mathcal{E}_0 = & \frac{-g}{2\pi} \int_0^\infty \frac{dp}{2\pi} \left\{ 2p^3 [C(p) - C_0(p)] + 2p^2 m_0 [S(p) - S_0(p)] \right. \\
& + \sigma \int_0^\infty \frac{dk}{2\pi} I_A(k, p, \mu) [S(k)S(p) - S_0(k)S_0(p)] \\
& \left. + I_B(k, p, \mu) [C(p)C(k) - C_0(k)C_0(p)] \right\}. \tag{19}
\end{aligned}$$

where  $\mathcal{E}_0$  is constant, and where we use the subindex  $_0$  when the mass  $m(p)$  is substituted by the constant current mass  $m_0$ . These two Eqs. (18) and (19) constitute the main object of our study.

### 3 Solving the mass gap equation variationally with rational ansatze

#### 3.1 Accurate numerical cancellation of infrared and ultraviolet divergences

We use both Eq. (18) and the minimization of Eq. (19) to find the dynamical quark mass  $m(k)$ , but first we must regulate correctly their divergences. The infrared divergences are present in the term  $pk/[(p-k)^2 + \mu^2]$ , infrared divergent in the limit of a vanishing regulator  $\mu \rightarrow 0$ , which is present both in the functions  $I_A(k, p, \mu)$  and  $I_B(k, p, \mu)$ . We must show that this infrared divergence is cancelled both in the fixed point Eq. (18) and in the energy density Eq. (19). In what concerns the fixed point Eq. (18), while the denominator diverges quadratically in  $1/(k-p)^2$ , the numerator  $m(k)p - m(p)k$  is of order  $(k-p)$  and thus the integrand diverges like  $1/(p-k)$  only, and its integral has finite principal value. In the energy density difference the infrared divergence also cancels, since the numerator common to the infrared divergent terms,

$$\begin{aligned}
& S(p)S(k) - S_0(p)S_0(k) + C(p)C(k) - C_0(p)C_0(k) \\
& = -\frac{1}{2} \times [\varphi'^2(p) - \varphi_0'^2(p)](k-p)^2 \\
& \quad - \frac{1}{2} [\varphi'(p)\varphi''(p) - \varphi_0'(p)\varphi_0''(p)](k-p)^3 + o(p-k)^4
\end{aligned} \tag{20}$$

is then of order  $(k-p)^2$ .

In the ultraviolet part of the integrals, while each sub-term in the propagator function integrands  $I_A(k, p, \mu)$  and  $I_B(k, p, \mu)$  is divergent, the actual sum is ultraviolet convergent, since in the limit of large  $k$  we have,



$$\begin{aligned}
p I_A(k, p, 0) &= \sum_{n=1}^{\infty} 4n \frac{p^{2n+1}}{k^{2n}} , \\
k I_B(k, p, \mu) &= \sum_{n=1}^{\infty} 4n \left( \frac{n+1}{n+\frac{1}{2}} \right) \frac{p^{2n+1}}{k^{2n}} ,
\end{aligned} \tag{21}$$

and thus the integrals in  $k$  have ultraviolet integrable integrands decaying like  $p^3/k^2$ . Also, the ultraviolet divergence in the kinetic terms of the energy density  $2p^3 C(p) + 2p^2 m_0 S(p)$  cancels due to the difference with  $2p^3 C_0(p) + 2p^2 m_0 S_0(p)$  if the mass difference  $m(k) - m_0$  vanishes sufficiently fast in the ultraviolet.

To address correctly both the infrared and ultraviolet divergences of the integrals in  $k$  of Eqs. (18) and (19), we divide the integral in two sections, the infrared one for  $0 < k < 2p$  and the ultraviolet one for  $2p < k < \infty$ . In the infrared region we compute the respective principal value, performing a symmetric sum centred in  $k = p$ , maintaining a very small regulator  $\mu$  just to cancel automatically the contribution of  $k = p$ . In the ultraviolet region we use the change of variable [33] of Adler and Davis  $k \rightarrow x/(1-x)$  with Jacobian  $1/(1-x)^2$  and with integration between  $x = 2p/(1+2p)$  and 1. The change of variable in the ultraviolet transforms, say an integral of rational functions  $1/(1+k)^n$  into the integral of polynomials  $(1-x)^{n-2}$  and thus it is adequate to the integral of rational functions as we have here. Our numerical integrals in  $k$  of a generic integrand  $\mathcal{I}$  singular in  $p$  are thus computed in the form,

$$\int_0^{\infty} dk \mathcal{I}(k) = \text{P} \left[ \int_0^{2p} dk \mathcal{I}(k) \right] + \int_{\frac{2p}{1+2p}}^1 \frac{dx}{(1-x)^2} \mathcal{I} \left( \frac{x}{1-x} \right) , \tag{22}$$

where each of the two numerical integrals can either be computed with a rectangular, trapezoidal or Simpson sum or with the gauss quadrature method.

If one would discretize the quark mass  $m(p)$  in a series of momenta  $p_i$ , then the integrals of Eq. (22) loses accuracy. Finite differences would require many interpolations, both in the infrared end and in the ultraviolet end, since the principal value requires that  $k$  has many summation points smaller than  $p$  and many other larger than  $p$ . Moreover the correct integration of the integrand in the ultraviolet large  $k$  limit, where the integrand behaves like  $\left(\frac{p}{k}\right)^2$ , also requires an integration extending beyond any value of  $p$ . To solve this problem, we utilize a well defined ansatz for  $m(k)$ , formally describe the parametrized as,

$$m(p) = m(p; c_1, c_2, \dots, c_n) . \tag{23}$$

and this allows the numerical summation for the integrals in any point of the

integration domain.

In what concerns the numerical convergence to the solution for  $m(k)$ , the fixed point equation is relatively unstable, particularly in the infrared region of  $p \simeq 0$ , when we are searching for the vacuum groundstate. Notice that the mass gap equation had not only one, but an infinite tower of solutions [38]. The excited solutions dominate the fixed point iteration, converging to the larger eigenvalue of the iterated matrix, because they minimize the denominator  $\sqrt{k^2 + m^2}$ . Previously in the literature, the fixed point method was provided with extra stability with two different methods, Adler and Davis used a cubic equation and relaxation, to select the best solution [33]. Bicudo and Nefediev quasi-linearized the fixed point equation and selected the desired eigenvalue, corresponding either to the stable vacuum or to excited, false vacua [38]. Thus they were able to find both the stable vacuum and the excited false vacua. But these works have not yet determined in detail  $m(0)$ , since this demands a very large numerical precision, and since most previous authors have focused in computing the function  $S(p)$  which in the infrared region is  $S(0) = 1$  regardless of the actual finite value of  $m(0)$ . Importantly, the present technique of minimizing the energy density directly tends to the right solution, which is the groundstate vacuum.

Interestingly, the variation of the ansatz parameters  $c_1, c_2, \dots, c_n$  of the energy density of the vacuum  $\mathcal{E} = \mathcal{E}(c_1, c_2, \dots, c_n)$  utilized in minimization codes with gradient method, utilizes the fixed point equation. Computing the partial derivatives of the energy density we get,

$$\begin{aligned} \frac{\partial \mathcal{E}(c_i)}{\partial c_i} &= \int dp \frac{\delta \mathcal{E}}{\delta \varphi} \frac{\partial \varphi}{\partial c_i} \\ &= -\frac{g}{2\pi} \int_0^\infty \frac{dp}{2\pi} (-2p^2) \mathcal{R}(p; c_i) \frac{p}{p^2 + m^2(p; c_i)} \frac{\partial m(p; c_i)}{\partial c_i}, \end{aligned} \quad (24)$$

where  $\mathcal{R}(p; c_i)$  is the right hand side of the mass gap Eq. (8),

$$\mathcal{R}(p; c_i) = +S(p; c_i)B(p; c_i) - C(p; c_i)A(p; c_i), \quad (25)$$

utilized in the fixed point Eq. (18).

### 3.2 Choosing variational ansatze for the quark mass $m(p)$

To guide our choice of ansatze  $m(p; c_1, c_2, \dots, c_n)$ , we first notice that the series expansion for  $I_A$  and  $I_B$  in Eq. (21), also apply when  $k \leftrightarrow p$ . When replaced in the integral of the fixed point equation (18), the series suggest that a series

expansion of  $m(p)$  should only have even terms, *i. e.*  $m(p)$  should be a function of  $p^2$ .  $m(p)$  should also be a finite function since our integrals are finite.

In what concerns the asymptotic ultraviolet tail of the integral of the fixed point equation (18), there are two different limits we can address. In the case of a large current quark mass  $m_0$ ,  $\frac{m_0}{k^2+m_0^2}$  interpolates between 1 in the infrared region of the integral and  $\frac{m_0}{k}$  in the ultraviolet region of the integral. Using these approximation, the components of the integral are analytical,

$$\begin{aligned}
\int_0^\infty \frac{dk}{2\pi} p I_A(k, p, \mu) &= \frac{p^3}{2\mu} , \\
\int_0^\infty \frac{dk}{2\pi} k I_B(k, p, \mu) &= \frac{p^3}{2\mu} , \\
\int_0^\infty \frac{dk}{2\pi} \frac{p}{k} I_A(k, p, \mu) &= \frac{p^2 \arctan \frac{p}{\mu}}{\pi \mu} \\
&= \frac{p^2}{2\mu} - \frac{p}{\pi} + o(\mu) , \\
\int_0^\infty \frac{dk}{2\pi} I_B(k, p, \mu) &= \frac{-p\mu + (p^2 + \mu^2) \arctan \frac{p}{\mu}}{\pi \mu} \\
&= \frac{p^2}{2\mu} - 2\frac{p}{\pi} + o(\mu) ,
\end{aligned} \tag{26}$$

and thus adding the respective components we find that in the infrared dominated approximation the integrals cancel, while in the ultraviolet dominated approximation the integral with  $\frac{m_0}{k}$  produces an ultraviolet behaviour of  $m(p) - m_0 \rightarrow \frac{m_0 \sigma}{\pi p^2}$ . Thus in the case of large  $m_0$  we expect that  $m(p) - m_0$  decays in the ultraviolet like  $1/p^2$ .

In the case where  $m_0 \simeq 0$ , assuming then that in the large  $p$  limit the dynamical quark mass vanishes sufficiently fast, the fixed point equation leads to,

$$\begin{aligned}
m(p) &\rightarrow \frac{\sigma}{p^3} \int_0^\infty \frac{dk}{2\pi} \frac{1}{\sqrt{k^2 + m(k)^2}} 4 \frac{k^2}{p^2} m(k) p \\
&\rightarrow \frac{4\sigma}{p^4} \int_0^\infty \frac{dk}{2\pi} \frac{k^2 m(k)}{\sqrt{k^2 + m(k)^2}}
\end{aligned} \tag{27}$$

and, providing  $m(p)$  decays faster than  $1/p^2$  for a finite integral, this decays in the ultraviolet like  $1/p^4$ .

The simplest possible ansatz for  $m(p) - m_0$  we may have, function of  $p^2$ , and encompassing both the behaviour in  $1/p^2$  for a large current quark mass  $m_0$  and the behaviour in  $1/p^4$  for a small current quark mass is the rational function,

$$\mathcal{A}_3(p) = \frac{1}{c_0 + c_2 p^2 + c_4 p^4} . \quad (28)$$

This ansatz is a Padé approximant, and to check whether our simple ansatz is sufficient, it is convenient to check that the next Padé approximant, a more flexible rational ansatz with two more parameters,

$$\mathcal{A}_5(p) = \frac{1 + n_2 p^2}{d_0 + d_2 p^2 + d_4 p^4 + d_6 p^6} \quad (29)$$

leads to the same result. In both ansatze of Eq. (28) and Eq. (29) we assume that the parameters are positive. While Eq. (28) is a decreasing function, Eq. (29) may have a different behaviour at the origin, either with an initial increase, or with a steeper decrease, and thus it has room in its parameter space to verify if the ansatz of Eq. (28) is close to the correct solution of the mass gap equation.

We also check numerically that ansatze with steeper infrared behaviours, including in the denominator terms like a  $c_1 k$  or a  $c_{-1}/k$  would not improve the solution since the best solution would have  $c_1 = c_{-1} = 0$ . A better ansatz than  $\mathcal{A}_3(p)$  is  $\mathcal{A}_5(p)$ , however the improvement of the solution is very small, almost invisible to the naked eye in graphics. The partial redundancy between the numerator and denominator parameters of  $\mathcal{A}_5(p)$  already slows the convergence to the minimum of the energy density  $\mathcal{E}$ . Thus an ansatz with more parameters than  $\mathcal{A}_5(p)$  is not necessary. The only ansatze we adopt here are the ones of the rational functions  $\mathcal{A}_3(p)$  and  $\mathcal{A}_5(p)$ .

### 3.3 One loop results for the large current mass $m_0 \gg \sqrt{\sigma}$ limit

We now compute the first iteration of the fixed point method starting with  $m(k) = m_0$ . In the simple case of a constant mass  $m(k) = m_0$ , we can compute the integral in the fixed point equation with a large precision. Defining the mass difference  $\mathcal{D}$ ,

$$\mathcal{D}(p) = m(p) - m_0 , \quad (30)$$

we compute  $\mathcal{D}(p)$  in the case a constant mass  $m_0$  is used in the integrand,

$$\mathcal{D}_0(p) = \frac{m_0 \sigma}{p^3} \int_0^\infty \frac{dk}{2\pi} \frac{I_A(k, p, \mu) p - I_B(k, p, \mu) k}{\sqrt{k^2 + m_0^2}}. \quad (31)$$

We get an accurate result for the integral  $\mathcal{D}_0(p)$ , with a numerical integration decomposed according to Eq. (22).

This provides a good quark mass solution to  $m(p) = m_0 + \mathcal{D}(p)$  whenever the current quark mass is large, i. e. when  $m_0 \gg \mathcal{D}(p)$ . In that case the integral  $\mathcal{D}_0(p)$  only needs to be computed once, since this one-loop approximation is already excellent.

Moreover we can rescale in  $m_0$ , and then with a single computation we get  $m(p)$  for any constant mass  $m_0$ . Denoting  $\tilde{k} = k/m_0$  and so forth we get,

$$\begin{aligned} \mathcal{D}_0(p) &= \frac{\sigma}{m_0 \tilde{p}^3} \int_0^\infty \frac{d\tilde{k}}{2\pi} \frac{I_A(\tilde{k}, \tilde{p}, \tilde{\mu}) \tilde{p} - I_B(\tilde{k}, \tilde{p}, \tilde{\mu}) \tilde{k}}{\sqrt{\tilde{k}^2 + 1}} \\ &= \frac{\sigma}{m_0} \mathcal{F}\left(\frac{p}{m_0}\right), \\ \mathcal{F}(p) &= \frac{1}{p^3} \int_0^\infty \frac{dk}{2\pi} \frac{I_A(k, p, \mu) p - I_B(k, p, \mu) k}{\sqrt{k^2 + 1}}. \end{aligned} \quad (32)$$

Thus we only need to compute the dimensionless function  $\mathcal{F}(p)$  and this will produce the dynamical quark mass for any current quark mass  $m_0$  larger than the typical scale  $\sqrt{\sigma}$  of our problem,

$$m(p) \simeq m_0 + \frac{\sigma}{m_0} \mathcal{F}\left(\frac{p}{m_0}\right). \quad (33)$$

The solution of the integration, obtained with the simplest numerical rectangular sum in both integrals, but needing  $10^3$  integration points at least, is represented in Fig. 1.

To be able to perform an accurate integration both in the infrared and the ultraviolet, it is necessary to have an analytical function. We obtain an analytical function by fitting the function  $\mathcal{F}(p)$ , and we get an excellent fit already with the very simple ansatz  $\mathcal{A}_3(p)$  of Eq. (28) for the parameter set,

$$c_0 = 4.7664, \quad c_2 = 3.4762, \quad c_4 = 0.0000, \quad (34)$$

with almost no graphically visible difference in Fig. 1 from the ansatz  $\mathcal{A}_5(p)$  with two more parameters of Eq. (29) for the parameter set,

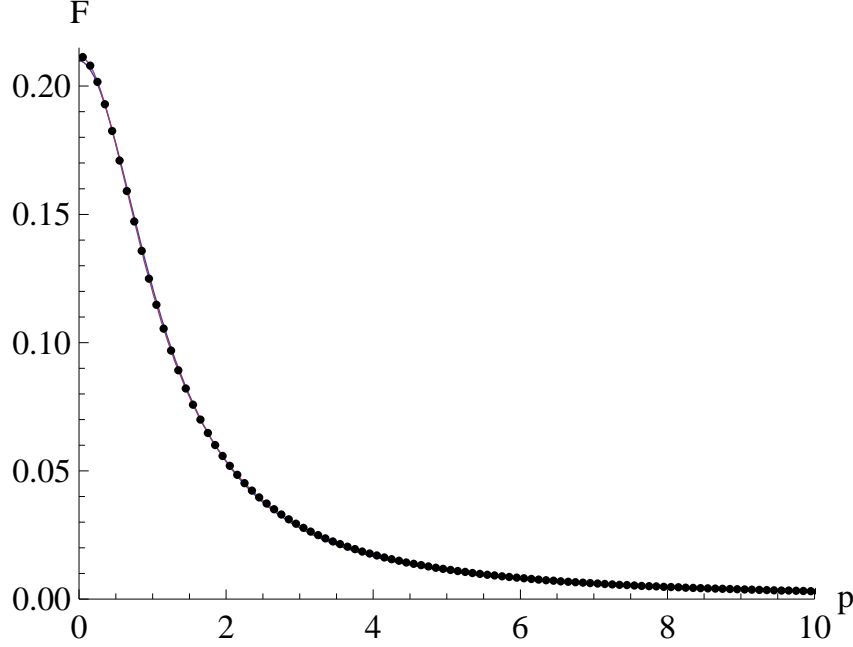


Fig. 1. Dimensionless mass difference function  $\mathcal{F}(\tilde{p})$  computed in the limit when the current quark mass  $m_0$  is large. The dots show the numerical integral of Eq. (32) and the two almost overlapping solid lines show our fits with the two different rational ansatze of Eq. (28) and Eq. (29).

$$d_0 = 4.7250, \quad d_2 = 4.9818, \quad d_4 = 0.8392, \quad d_6 = 0.0000, \quad n_2 = 0.2626, \quad (35)$$

and both fits confirm the  $1/p^2$  decay of the mass in the ultraviolet, for large current quark masses.

Now we can include the large quark limit scaling in  $m_0$ , and also apply to the quark mass difference  $\mathcal{D}_0(p)$  the ansatz  $\mathcal{A}_3(p)$  of Eq. (28), and in this case the ansatz parameters should be respectively,

$$c_0 = 4.7664 m_0, \quad c_2 = 3.4762 m_0^{-1}, \quad c_4 = 0.0000 m_0^{-3}. \quad (36)$$

We further compute the vacuum energy density difference for a large current quark mass  $m_0$ . Although the mass difference  $\mathcal{D}_0(p)$  in Eq. (32) decreases like  $m_0^{-1}$  in the large current quark mass  $m_0$  limit, a dimensional analysis of  $\mathcal{E} - \mathcal{E}_0$  shows that possibly it does not vanish. Since the energy difference is finite and independent of the infrared cutoff  $\mu$ , then our only dimensionfull parameters are the string tension  $\sigma$  (scaling like a mass square) and the current quark mass  $m_0$  (scaling like a mass). Because the vacuum energy density per volume scales like a mass to the fourth power, a large mass expansion may have terms of the form  $m_0^4, m_0^2\sigma, \sigma^2, \sigma^3 m_0^{-2}, \dots$ . However the first term in this series clearly vanishes in the vacuum energy difference  $\mathcal{E} - \mathcal{E}_0$ . Then the question is what is the first non-vanishing term in this expansion.

| $m_0$       | $10^4 \frac{\mathcal{E} - \mathcal{E}_0}{g}$ | $c_0$   | $c_2$    | $c_4$    |
|-------------|--|---------|----------|----------|
| 0.000100000 | -0.473813                                    | 6.24900 | 26.7910  | 17.5059  |
| 0.000316228 | -0.478133                                    | 6.24287 | 26.7090  | 17.3392  |
| 0.00100000  | -0.491581                                    | 6.22441 | 26.4168  | 16.8674  |
| 0.00316228  | -0.532245                                    | 6.17597 | 25.4076  | 15.8086  |
| 0.0100000   | -0.649468                                    | 6.01623 | 23.2517  | 12.0965  |
| 0.0316228   | -0.958565                                    | 5.68682 | 18.5897  | 6.38068  |
| 0.100000    | -1.62048                                     | 5.22374 | 12.5110  | 1.50433  |
| 0.316228    | -2.58117                                     | 5.04452 | 7.22212  | 0.051756 |
| 1.00000     | -3.27613                                     | 7.03428 | 3.06500  | 0.000000 |
| 3.16228     | -3.46213                                     | 17.1365 | 1.04266  | 0.000000 |
| 10.0000     | -3.47122                                     | 51.7243 | 0.336172 | 0.000000 |
| 31.6228     | -3.39336                                     | 153.536 | 0.113085 | 0.000000 |

Table 1

The results for the ansatz parameters of  $\mathcal{A}_3(p)$  for  $m(p) - m_0$  obtained with our minimization code. All results are in dimensionless units of  $\sigma = 0.19 \text{ GeV}^2 = 1$ .

To answer this question, we expand the vacuum energy density in a  $\frac{\sigma}{m_0^2}$  series, similar to the variation in Eq. (24), but now based in the expansion of the quark dynamical mass,

$$m(p) = m_0 + \frac{\sigma}{m_0} m_1 \left( \frac{p}{m_0} \right) + \frac{\sigma^2}{m_0^3} m_2 \left( \frac{p}{m_0} \right) + \dots \quad (37)$$

and then we get

$$\begin{aligned} \mathcal{E} = & \frac{-g}{2\pi} \int_0^\infty \frac{dp}{2\pi} \left\{ 2p^2 \left[ pC_0(p) + m_0 S_0(p) + \frac{p\delta C_0(p) + m_0 \delta S_0(p)}{\delta m_0} (m(p) - m_0) \right. \right. \\ & \left. \left. + \frac{1}{2} \frac{p\delta^2 C(p) + m_0 \delta^2 S_0(p)}{\delta m_0^2} (m(p) - m_0)^2 + \dots \right] \right. \\ & + \sigma \int_0^\infty \frac{dk}{2\pi} I_A(k, p, \mu) \left[ S_0(p) S_0(k) + 2 \frac{\delta S_0(p)}{\delta m_0} S_0(k) (m(p) - m_0) + \dots \right] \\ & \left. + I_B(k, p, \mu) \left[ C_0(p) C_0(k) + 2 \frac{\delta C_0(p)}{\delta m_0} C_0(k) (m(p) - m_0) + \dots \right] \right\}. \end{aligned} \quad (38)$$

The zeroth order term vanishes when we perform the difference of the vacuum energy densities  $\mathcal{E} - \mathcal{E}_0$ . Then the first order term in the kinetic energy density

| $m_0$       | $10^4 \frac{\mathcal{E} - \mathcal{E}_0}{g}$ | $d_0$  | $d_2$  | $d_4$  | $d_6$  | $n_2$  |
|-------------|--|--------|--------|--------|--------|--------|
| 0.000100000 | -0.473908                                    | 6.170  | 31.9   | 22.    | 14.    | 0.5    |
| 0.000316228 | -0.478221                                    | 6.163  | 32.3   | 23.    | 15.    | 0.6    |
| 0.00100000  | -0.491647                                    | 6.147  | 32.2   | 24.    | 16.    | 0.6    |
| 0.00316228  | -0.532266                                    | 6.09   | 33.1   | 30.    | 19.    | 0.9    |
| 0.0100000   | -0.649397                                    | 5.9705 | 29.582 | 28.37  | 12.83  | 0.871  |
| 0.0316228   | -0.958497                                    | 5.7202 | 25.358 | 32.40  | 7.4897 | 1.301  |
| 0.100000    | -1.624761                                    | 5.369  | 11.875 | 5.05   | 0.0000 | 0.149  |
| 0.316228    | -2.59104                                     | 5.467  | 6.720  | 2.08   | 0.0000 | 0.205  |
| 1.00000     | -3.27722                                     | 7.5349 | 4.4398 | 0.8105 | 0.0000 | 0.2546 |
| 3.16228     | -3.46240                                     | 16.665 | 1.2612 | 0.0105 | 0.0000 | 0.0104 |
| 10.0000     | -3.47148                                     | 49.    | 0.6    | 0.00   | 0.0000 | 0.00   |
| 31.6228     | -3.76155                                     | 92.    | 0.2    | 0.0000 | 0.0000 | 0.0000 |

Table 2

The results for the ansatz parameters of  $\mathcal{A}_5(p)$  for  $m(p) - m_0$  obtained with our minimization code. All results are in dimensionless units of  $\sigma = 0.19 \text{ GeV}^2 = 1$ .

also vanishes since the kinetic energy density is minimized by  $m(p) = m_0$ . Thus the leading term is of second order in the kinetic energy density, and of first order in the potential energy density, and both are proportional to  $\sigma^2$ . Using the intermediate steps,

$$\begin{aligned}
\frac{p\delta^2 C_0(p) + m_0\delta^2 S_0(p)}{\delta m_0^2} &= -\frac{p^2}{(p^2 + m_0^2)^{3/2}}, \\
\sigma \int_0^\infty \frac{dk}{2\pi} \left[ \frac{2\delta S_0(p)}{\delta m_0} I_A(k, p, \mu) S_0(k) + I_B(k, p, \mu) C_0(k) \right] \frac{2\delta C_0(p)}{\delta m_0} \\
&= 2 \frac{p^4}{(p^2 + m_0^2)^{3/2}} \frac{\sigma}{m_0} D_0\left(\frac{p}{m_0}\right),
\end{aligned} \tag{39}$$

and changing variable to the dimensionless  $\tilde{p}$ , we get,

$$\mathcal{E} - \mathcal{E}_0 = \sigma^2 \frac{-g}{2\pi} \int_0^\infty \frac{d\tilde{p}}{2\pi} \frac{\tilde{p}^4 [\mathcal{F}(\tilde{p})]^2}{(\tilde{p}^2 + 1)^{\frac{7}{2}}} + o\left(\frac{\sigma^3}{m_0^2}\right). \tag{40}$$

Finally using the ansatz  $\mathcal{A}_3(p)$  of Eq. (28), with the parameter set of Eq. (34) this results in



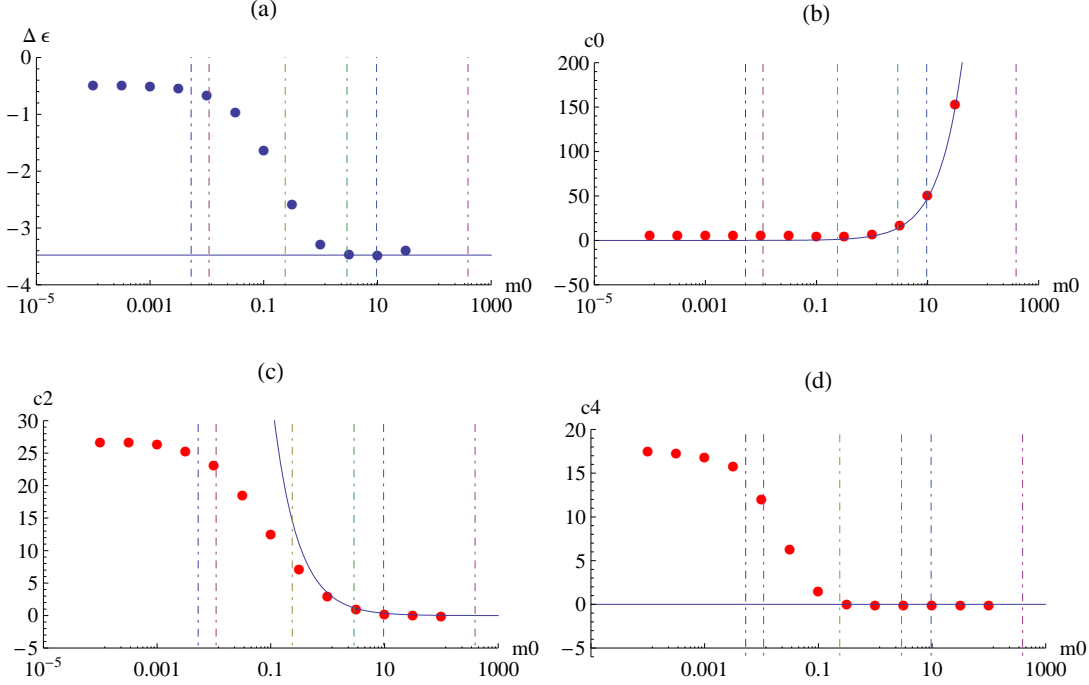


Fig. 2. Plots of our numerical solution with the ansatz  $\mathcal{A}_3(p)$ , as a function of the current quark mass  $m_0$ : (a) the vacuum energy density shift  $\mathcal{E} - \mathcal{E}_0$ , (b) parameter  $c_0$ , (c) parameter  $c_2$ , (d) Parameter  $c_4$ . The dots show our numerical solution, the solid line is the large  $m_0$  limit obtained with Eqs. (36) and (41), and the vertical dot-dashed lines represent the current masses of the quarks  $u, d, s, c, b, t$ .

$$\mathcal{E} - \mathcal{E}_0 \simeq - 3.47701 \times 10^{-4} \sigma^2 g . \quad (41)$$

## 4 Results

Utilizing our ansatz of Eq. (28) and Eq. (29), we may now compute with great accuracy the integrals of Eq. (19) which now are a function of the ansatz parameters, and apply a standard minimizing code to determine the optimal parameters. We use  $1000 \times 1000$  integration points and up to 40 decimal digits in order to be able to find a convergence of the method in the case of the ansatz  $\mathcal{A}_5(p)$ , due to the partial redundancy of the parameters. Then we also minimize the energy starting from different randomly generated initial values for the parameters. In Tables 1 and 2 we only show the digits which are stable, in the sense that they do not depend on the initial values. Notice that the energy density obtained with the two different ansatze differ only by a few per mil and that the ansatz of Eq. (29) already exhibits some redundancy in the parameters. This shows that the ansatz of Eq. (28) is already quite accurate for the parametrization of the quark mass  $m(p)$ .

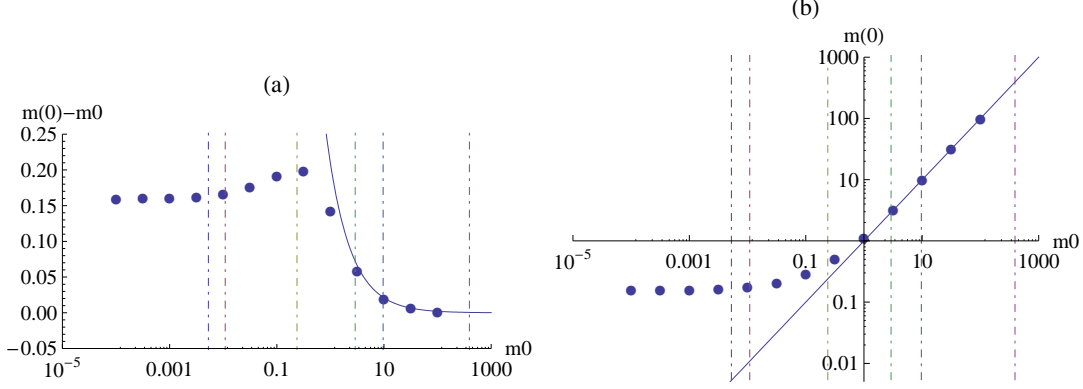


Fig. 3. Plots of the mass gap as a function of the current quark mass  $m_0$ : (a) the mass gap difference  $m(0) - m_0$ , measuring the amount of generated dynamical mass, (b) the mass gap  $m(0)$ . The dots show our numerical solution, the solid line is the leading order obtained when  $m_0 \rightarrow \infty$ , and the vertical dot-dashed lines represent the current masses of the quarks  $u, d, s, c, b, t$ . Notice that the dynamical mass generation has a maximum for finite quark masses close to the strange quark mass. All results are in dimensionless units of  $\sigma = 0.19 \text{ GeV}^2 = 1$ .

Unlike the fixed point method, converging quite fast (with a single iteration) for large current quark masses  $m_0 \gg \sqrt{\sigma}$ , the variational method converges faster for small current quark masses. Thus both methods are complementary. In Tables 1 and 2 and in Fig. 2 we show the results of our minimization for two ansatz and for different current quark masses spanning over five orders of magnitude. In Figs. 3 and 4 we illustrate the mass difference at the momentum origin  $m(0) - m_0$ , the mass gap  $m(0)$  and the running mass  $m(p)$  for different current masses  $m_0$ .

Now that we have an excellent and simple ansatz for the running quark mass, we may compute the regularized quark condensate and the quark dispersion relation. The quark condensate  $\langle \bar{\psi}\psi \rangle$  is another possible order parameter, to be compared with the other order parameter we computed, *i. e.* the quark mass at vanishing momentum  $m(0)$ . The quark condensate is computed from the one-loop quark propagator functions in Eq. (10), and it is ultraviolet divergent for finite quark masses. Thus we regularize the quark condensate, subtracting the quark condensate for a current quark,

$$\langle \bar{\psi}\psi \rangle - \langle \bar{\psi}\psi \rangle_0 = -\frac{g}{\pi^2} \int_0^\infty k^2 dk \left[ \frac{m(k)}{\sqrt{k^2 + m(k)^2}} - \frac{m_0}{\sqrt{k^2 + m_0^2}} \right] \quad (42)$$

The one quark dispersion relation  $E(p)$ , defined in Eq. (9), is relevant for the boundstate equation of mesons or of baryons. For instance, in the instantaneous Salpeter equation, a hamiltonian  $H = E_q + E_{\bar{q}} + V_{q\bar{q}}$  can be defined for mesons (actually the hamiltonian is a matrix [37] including negative and

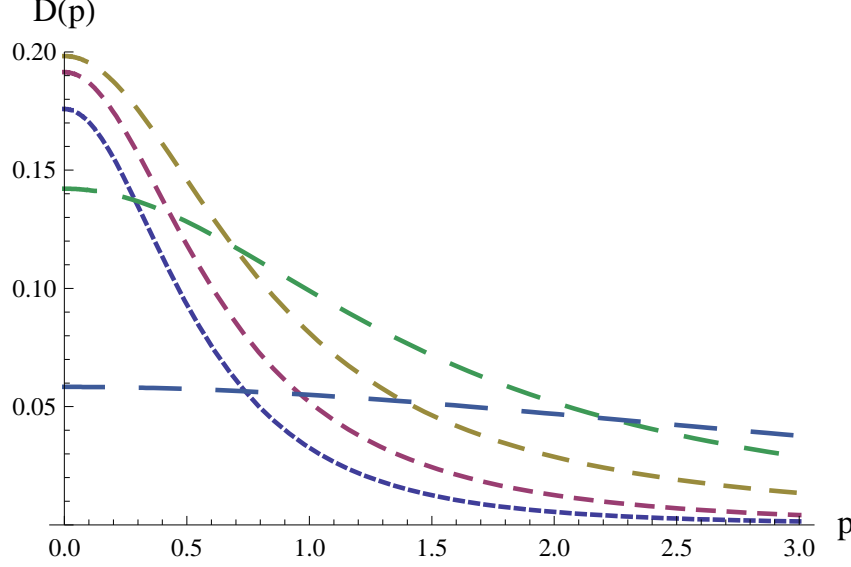


Fig. 4. The quark mass function difference  $\mathcal{D}(p) = m(p) - m_0$  measuring the extent of dynamical mass generation, is represented with increasing number of dashes per curve for five different current quark masses  $m_0$  with values  $10^{-4}, 10^{-1}, 10^{-1/2}, 10^0, 10^{1/2}$ , in dimensionless units of  $\sigma = 0.19 \text{ GeV}^2 = 1$ .

positive energy components). The dispersion relation  $E(p)$  is infrared divergent due to the infinite constant of quark-antiquark potential detailed in Eq. (12). In momentum space, this leads to an infinite Dirac delta in the integral present in  $E(p)$ . We can regularize the numerical integral, subtracting a term to cancel the integrand when  $k = p$ , a term that we add back analytically,

$$E(p) = pC(p) + m_0S(p) + \frac{\sigma}{p^2} \int_0^\infty \frac{dk}{2\pi} \left\{ I_A(k, p, \mu) [S(k) - S(p)] S(p) \right. \quad (43) \\ \left. + I_B(k, p, \mu) [C(p) - C(k)] C(k) + [I_A(k, p, \mu) S^2(p) + I_B(k, p, \mu) C^2(p)] \right\},$$

in particular the integral of  $I_A S^2 + I_B C^2$  is analytical thanks to Eq. (26), and in the limit of a vanishing infrared regulator  $\mu \rightarrow 0$  this term, that we subtracted and must now add back to the quark energy, reduces to a simple infrared divergence plus a finite term,

$$\frac{\sigma}{p^2} \int_0^\infty \frac{dk}{2\pi} I_A(k, p, \mu) S^2(p) + I_B(k, p, \mu) C^2(p) \rightarrow \frac{\sigma}{2\mu} - \frac{2\sigma}{\pi} \frac{p}{p^2 - m(p)^2}. \quad (44)$$

Importantly, this divergence is physically irrelevant since, in the hamiltonian of any colour singlet hadron, the sum of the divergences of the quark and of the antiquark energies cancel with the infrared divergence of the quark-antiquark potential detailed in Eq. (12). Finally for the purpose of future computations

| $m_0$       | $\left(\frac{-\langle\bar{\psi}\psi\rangle+\langle\bar{\psi}\psi\rangle_0}{g}\right)^{\frac{1}{4}}$ | $e_0$   | $e_1$  | $e_3$   | $e_5$  |
|-------------|---|---------|--------|---------|--------|
| 0.000100000 | 0.255569  | 0.21104 | 1.9549 | 102.65  | 451.90 |
| 0.000316228 | 0.255847  | 0.21156 | 1.9539 | 102.23  | 448.34 |
| 0.00100000  | 0.256701  | 0.21321 | 1.9518 | 100.94  | 436.59 |
| 0.00316228  | 0.259029  | 0.21814 | 1.9488 | 97.304  | 399.80 |
| 0.0100000   | 0.267020  | 0.23387 | 1.9269 | 86.717  | 317.83 |
| 0.0316228   | 0.287014  | 0.27830 | 1.8859 | 65.176  | 173.48 |
| 0.100000    | 0.331664  | 0.39429 | 1.8758 | 35.484  | 49.785 |
| 0.316228    | 0.428943  | 0.71809 | 1.8628 | 13.582  | 3.6035 |
| 1.00000     | 0.771803  | 1.6210  | 2.2704 | 2.8947  | 0.0076 |
| 3.16228     | 0.984801  | 4.7134  | 2.4773 | 0.34516 | 0.0000 |
| 10.0000     | 1.26682   | 14.999  | 2.4199 | 0.03598 | 0.0000 |
| 31.6228     | 1.60590   | 48.113  | 2.3283 | 0.00371 | 0.0000 |

Table 3

The results for the regularized quark condensate and for the regularized quark dispersion relation obtained with the ansatz of Eq. (46). All results are in dimensionless units of  $\sigma = 0.19 \text{ GeV}^2 = 1$ .

of the hadron spectra, it is convenient to write the dispersion relation as a sum of the analytical infrared term of Eq. (44), plus the free quark dispersion relation dominating the ultraviolet, and plus a finite and compact term  $\tilde{E}(p)$ , an integral that we compute numerically,

$$E(p) = \frac{\sigma}{2\mu} - \frac{2\sigma}{\pi} \frac{p}{p^2 - m(p)^2} + pC(p) + m_0S(p) + \tilde{E}(p) . \quad (45)$$

The numerical integral  $\tilde{E}(p)$  decays like  $1/p^5$  in the chiral limit of small current quark masses and decays like  $1/p^3$  in the case of large current quark masses.  $\tilde{E}(p)$  is negative and we can conveniently fit it with the rational function, or Padé approximant with odd powers of  $p$  only,

$$\tilde{E}(p) \simeq -\frac{1}{e_0 + e_1p + e_3p^3 + e_5p^5} . \quad (46)$$

We show the best fitting parameters  $e_0, e_1, e_3, e_5$  in Table 3. With our excellent fits of the dynamical quark mass  $m(p)$  and of the quark dispersion relation  $E(p)$  we are well equipped to address further problems, such as the breaking of chiral symmetry or the hadronic excited spectra at finite temperature  $T$ .

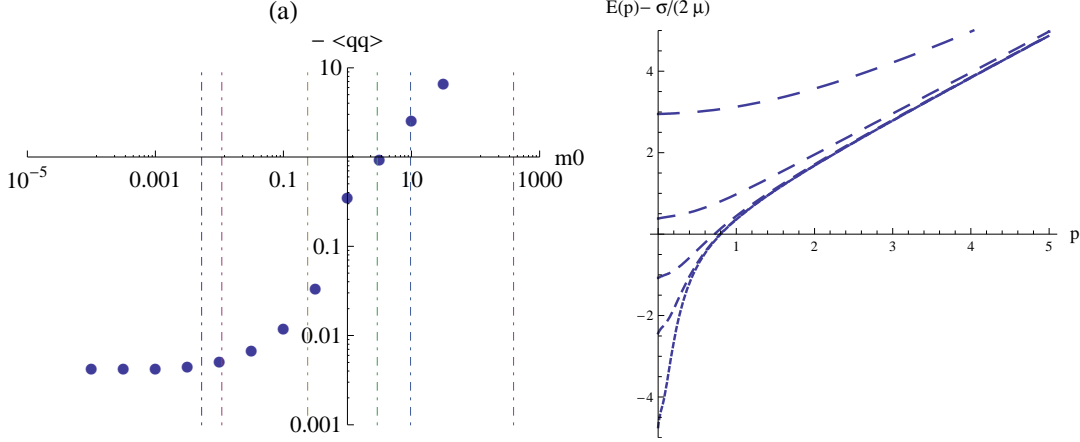


Fig. 5. (a) We show a log log plot of minus the regularized quark condensate  $-\langle\bar{\psi}\psi\rangle + \langle\bar{\psi}\psi\rangle_0$  as a function of the current quark mass  $m_0$ , with vertical dot-dashed lines representing the current masses of the quarks  $u, d, s, c, b, t$ . (b) We represent the regularized quark dispersion relation  $E(p) - \frac{\sigma}{2\mu}$  with increasing number of dashes per curve for five different current quark masses  $m_0$  with respective values  $10^{-4}, 10^{-1}, 10^{-1/2}, 10^0, 10^{1/2}$ . The quark condensate has an inflection point for finite quark masses close to the strange quark mass, and for large masses it rises linearly with  $m_0$ . All results are in dimensionless units of  $\sigma = 0.19 \text{ GeV}^2 = 1$ .

## 5 Conclusion

While the chiral limit of  $m_0 \ll \sqrt{\sigma}$  was already well known in the literature, we find unanticipated effects for finite  $m_0 \simeq \sqrt{\sigma}$  and for heavy  $m_0 \gg \sqrt{\sigma}$  current quark masses. We study in detail the large  $m_0$  limit, performing an one-loop expansion in the dimensionless number  $\sigma/m_0^2$ . We also develop a new technical approach to solve the mass gap equation, utilizing the variational principle to increase the precision of our mass solution  $m(p)$  in the infrared limit of  $p \rightarrow 0$ , relevant to compute the mass gap  $m(0)$ , an order parameter for the chiral phase transition. We also show that the dynamical generated constituent quark mass  $m(p)$  can be quite well fitted by our inverse even quartic polynomial ansatz, a Padé approximant with parameters  $c_0, c_2$  and  $c_4$  depending only on the current mass  $m_0$ .

Our surprising results are that the dynamical mass generation has finite effects persistent beyond the chiral limit. At  $m_0 \simeq \sqrt{\sigma}$ , in particular for masses similar to the strange quark  $s$  mass, the quark mass generation  $m(0) - m_0$  is maximum, as shown in Fig. 4, while one would naively expect the quark mass generation to be maximum in the chiral limit close to the up  $u$  or down  $d$  quark masses. A second order parameter, the regularized quark condensate  $\langle\bar{\psi}\psi\rangle - \langle\bar{\psi}\psi\rangle_0$ , monotonously grows in absolute value with  $m_0$  and shows an inflexion point for masses similar to the strange quark  $s$  mass, as depicted in Fig. 5. In the limit of heavy quark masses  $m_0 \gg \sqrt{\sigma}$  of the charm  $c$ , bottom  $b$  and top  $t$  quarks, although the mass gap difference  $m(0) - m_0$  vanishes like

$\sigma/m_0$ , it occurs that the energy density difference  $\mathcal{E} - \mathcal{E}_0$  is maximum. In the heavy quark limit, the energy density difference converges to a constant limit when  $m_0 \rightarrow \infty$ , and we show in Fig. 2 that it is one order of magnitude larger than in the chiral limit. This may be relevant for cosmology, contributing to the dark energy.

The numerical variational technique developed here, together with the detailed solutions for the running quark mass  $m(p)$  and for the quark dispersion relation  $E(p)$  as a function of the current quark mass  $m_0$  and of the string tension  $\sigma$ , are necessary tools for the continuation of our program to study the QCD phase diagram and the hadron spectrum at finite temperature  $T$  and density  $\mu$ , when the string tension  $\sigma$  becomes quite small, possibly smaller than the light current quark masses.

### acknowledgements

I am very grateful to Gastão Krein on the variational method, and to Marlene Nahrgang, to Pedro Sacramento and to Jan Pawłowski for discussions on the QCD phase diagram motivating this paper. I acknowledge the financial support of the FCT grants CFTP, CERN/ FP/ 109327/ 2009 and CERN/ FP/ 109307/ 2009.

### References

- [1] H. J. Munczek and A. M. Nemirovsky, Phys. Rev. D **28**, 181 (1983).
- [2] P. Jain and H. J. Munczek, Phys. Rev. D **44**, 1873 (1991).
- [3] H. J. Munczek and P. Jain, Phys. Rev. D **46**, 438 (1992).
- [4] P. Jain and H. J. Munczek, Phys. Rev. D **48**, 5403 (1993) [arXiv:hep-ph/9307221].
- [5] P. Bicudo and J. E. Ribeiro, Phys. Rev. D **42**, 1635 (1990).
- [6] P. Bicudo and J. E. Ribeiro, Phys. Rev. D **42**, 1625 (1990).
- [7] P. Bicudo and J. Ribeiro, Phys. Rev. D **42**, 1611 (1990).
- [8] F. J. Llanes-Estrada, S. R. Cotanch, Phys. Rev. Lett. **84**, 1102 (2000).
- [9] F. J. Llanes-Estrada, S. R. Cotanch, A. P. Szczepaniak and E. S. Swanson, Phys. Rev. C **70**, 035202 (2004) [arXiv:hep-ph/0402253].
- [10] P. Bicudo, M. Cardoso, T. Van Cauteren and F. J. Llanes-Estrada, Phys. Rev. Lett. **103**, 092003 (2009) [arXiv:0902.3613 [hep-ph]].
- [11] P. Bicudo, Phys. Rev. Lett. **72**, 1600 (1994).
- [12] O. A. Battistel and G. Krein, Mod. Phys. Lett. A **18**, 2255 (2003).

- [13] S. M. Antunes, G. Krein, V. E. Vizcarra and P. K. Panda, Braz. J. Phys. **35**, 877 (2005).
- [14] L. Y. Glozman and R. F. Wagenbrunn, Phys. Rev. D **77**, 054027 (2008) [arXiv:0709.3080 [hep-ph]].
- [15] P. Guo and A. P. Szczepaniak, Phys. Rev. D **79**, 116006 (2009) [arXiv:0902.1316 [hep-ph]].
- [16] P. M. Lo and E. S. Swanson, arXiv:0908.4099 [hep-ph].
- [17] T. Kojo, Y. Hidaka, L. McLerran and R. D. Pisarski, arXiv:0912.3800 [hep-ph].
- [18] A. V. Nefediev and J. E. F. Ribeiro, arXiv:0906.1288 [hep-ph].
- [19] T.D. Lee, Particle Physics and Introduction to Field Theory, (Harwood Academic Publishers, New York, 1981).
- [20] A. Szczepaniak, E. S. Swanson, C. R. Ji and S. R. Cotanch, Phys. Rev. Lett. **76**, 2011 (1996) [arXiv:hep-ph/9511422].
- [21] A. P. Szczepaniak and E. S. Swanson, Phys. Rev. D **55**, 1578 (1997) [arXiv:hep-ph/9609525].
- [22] I. I. Balitsky, Nucl. Phys. B **254**, 166 (1985).
- [23] H. G. Dosch, Phys. Lett. B **190**, 177 (1987).
- [24] H. G. Dosch and Yu. A. Simonov, Phys. Lett. B **205**, 339 (1988).
- [25] P. Bicudo, N. Brambilla, E. Ribeiro and A. Vairo, Phys. Lett. B **442**, 349 (1998) [arXiv:hep-ph/9807460].
- [26] P. Bicudo, Phys. Rev. D **79**, 094030 (2009) [arXiv:0811.0407 [hep-ph]].
- [27] J. R. Finger and J. E. Mandula, Nucl. Phys. B **199**, 168 (1982).
- [28] A. Le Yaouanc, L. Oliver, O. Pene, J. C. Raynal, Phys. Lett. **134B**, 249 (1984).
- [29] A. Amer, A. Le Yaouanc, L. Oliver, O. Pene and J.-C. Raynal, Phys. Rev. Lett. **50**, 87 (1983).
- [30] A. Le Yaouanc, L. Oliver, O. Pene and J.-C. Raynal, Phys. Rev. D **29**, 1233 (1984);
- [31] A. Le Yaouanc, L. Oliver, S. Ono, O. Pène and J. C. Raynal, Phys. Rev. D **31**, 137 (1985).
- [32] Y. L. Kalinovsky, L. Kaschluhn and V. N. Pervushin, Phys. Lett. B **231**, 288 (1989).
- [33] S. L. Adler, A. C. Davis, Nucl. Phys. B **244**, 469 (1984),
- [34] P. Bicudo, J. E. Ribeiro and J. Rodrigues, Phys. Rev. C **52**, 2144 (1995).
- [35] R. Horvat, D. Kekez, D. Palle and D. Klabucar, Z. Phys. C **68**, 303 (1995).

- [36] R. F. Wagenbrunn and L. Y. Glozman, Phys. Rev. D **75**, 036007 (2007) [arXiv:hep-ph/0701039].
- [37] P. Bicudo, Phys. Rev. C **60**, 035209 (1999).
- [38] P. Bicudo and A. V. Nefediev, Phys. Rev. D **68**, 065021 (2003) [arXiv:hep-ph/0307302].